Journal of the Korean Physical Society (2021) 78:476–481
https://doi.org/10.1007/s40042-021-00068-4

Online ISSN 1976-8524
Print ISSN 0374-4884

ORIGINAL PAPER

Stable chimeras of non-locally coupled Kuramoto–Sakaguchi oscillators in a finite array

Seungjae Lee[1] · **Young Sul Cho**[1]

Received: 19 October 2020 / Revised: 8 December 2020 / Accepted: 14 December 2020 / Published online: 4 February 2021

Abstract
We consider chimera states of coupled identical phase oscillators where some oscillators are phase synchronized (have the same phase) while others are desynchronized. Chimera states of non-locally coupled Kuramoto–Sakaguchi oscillators in arrays of finite size are known to be chaotic transients; after a transient time, all the oscillators are phase synchronized, with the transient time increasing exponentially with the number of oscillators. In this work, we consider a small array of six non-locally coupled Kuramoto–Sakaguchi oscillators and modify the range of the phase lag parameter to destabilize their complete phase synchronization. Under these circumstances, we observe a chimera state spontaneously formed by the partition of oscillators into two independently synchronizable clusters of both stable and unstable synchronous states. In the chimera state, the trajectory of the phase differences of the desynchronized oscillators relative to the synchronous cluster is a stable periodic orbit, and as a result, the chimera state is a stable but not long-lived transient. We observe the chimera state with random initial conditions in a restricted range of the phase lag parameter and clarify why the state is observable in the restricted range using Floquet theory for periodic orbit stability.

Keywords Chimera state · Cluster synchronization · Non-locally coupled Kuramoto–Sakaguchi oscillators

1 Introduction

The chimera state, a phenomenon where coupled identical oscillators are partitioned into coherent and incoherent subsets [1, 2], has been widely studied both theoretically [3–23] and experimentally [24–35] using various definitions of coherence and incoherence [36]. The first observation of a chimera state was in arrays of non-locally coupled Ginzburg–Landau oscillators [3]. In the state, oscillators in an array are partitioned into two domains: one composed of phase-locked (coherent) oscillators, and one composed of drifting (incoherent) oscillators. To understand the phenomenon analytically, researches have used non-locally coupled Kuramoto–Sakaguchi oscillators [37] in arrays with the phase lag parameter $\alpha \in (0, \pi/2)$ with which a stable chimera state has been shown to exist in the limit of an infinite number of oscillators $N \to \infty$ [4, 5, 20]. However, later the chimera state was reported to become chaotic transient with finite N [7, 8, 18], because the complete phase synchronization of all the oscillators is stable in the range $0 < \alpha < \pi/2$ such that the chimera state collapses to complete phase synchronization after a transient time. Here, the transient time increases exponentially with N [8, 21, 29], which is consistent with the analytical result that the chimera state is stable in the limit $N \to \infty$ [4, 5, 20].

In this paper, we consider an array of six non-locally coupled Kuramoto–Sakaguchi oscillators with the phase lag parameter $\alpha \in (\pi/2, \pi)$, where complete phase synchronization is unstable and thus avoided. With this setup, we observe a chimera state in which two oscillators are phase synchronized (coherent), while the other four oscillators are desynchronized (incoherent). Here, phase synchronization of the two oscillators is guaranteed, because they receive the same input from the other four oscillators due to permutation symmetry [17, 38–40]. Moreover, we show that all oscillators behave periodically with a common period, and as a result, the four incoherent oscillators maintain their desynchronization, thereby leading to the chimera state being a stable but not long-lived transient. We note that chimera states with $\alpha \in (0, \pi/2)$ would collapse rapidly for such a small number of oscillators ($N = 6$) [8, 21, 29].

✉ Young Sul Cho
yscho@jbnu.ac.kr

[1] Department of Physics, Jeonbuk National University, 54896 Jeonju, Korea

Several approaches using diverse systems have been used to find stable chimeras with finite N [9–11, 13–17, 31], including several claims that finite stable chimeras can be observed even in non-locally coupled Kuramoto–Sakaguchi oscillators with some values of α in the range $0 < \alpha < \pi/2$ [13, 16]. Our approach in this paper claims that the avoidance of complete phase synchronization is the key to observe a stable chimera state composed of a finite number of oscillators [17, 19, 22, 32].

The rest of this paper is organized as follows. In Sect. 2, we describe the dynamical system where we observe a chimera state, identify the underlying mechanism of its formation, and demonstrate the state's periodic behavior. In Sect. 3, we measure the basin stability [41] of the chimera state and other possible states in the system, and in Sect. 4, we discuss the chimera state from the perspective of frequency synchronization and show that it is a weak chimera state [9–12].

2 Observation of a stable finite-sized chimera state

2.1 Kuramoto–Sakaguchi oscillators in a given network

We consider the Kuramoto–Sakaguchi model of phase oscillators [37]. In this model, the time derivative of the phase of each oscillator in a network is given by

$$\dot{\phi}_i(t) = \omega_i + K \sum_{j=1}^{N} A_{ij} \sin(\phi_j(t) - \phi_i(t) + \alpha) \tag{1}$$

for global coupling strength $K > 0$ and phase lag parameter $\alpha \in (0, \pi)$, where $\phi_i \in [0, 2\pi)$ $(i = 1, \ldots, N)$ is the phase of the ith oscillator and A_{ij} is each entry of the $N \times N$ adjacency matrix $\mathbf{A}$ of the network. We let all oscillators be identical such that they have the same natural frequency $\omega_i = \omega$ for $\forall i$. If we use a rotating reference frame $\phi_i \to \phi_i + \omega t$ for $\forall i$ and time scaling $t \to t/K$, Eq. (1) has the form

$$\dot{\phi}_i(t) = \sum_{j=1}^{N} A_{ij} \sin(\phi_j(t) - \phi_i(t) + \alpha). \tag{2}$$

To observe a chimera state in a finite array of non-locally coupled identical oscillators, we use a network of $N = 6$, as depicted in Fig. 1a, where each oscillator is coupled with neighbors within distance two on the ring. In this paper, we use Eq. (2) with A_{ij} of the network to find the chimera state.

2.2 Partition of network oscillators into two independently synchronizable clusters

The six oscillators in Fig. 1a are partitioned into two clusters $C_1 = \{1, 4\}$ and $C_2 = \{2, 3, 5, 6\}$. We denote the synchronous

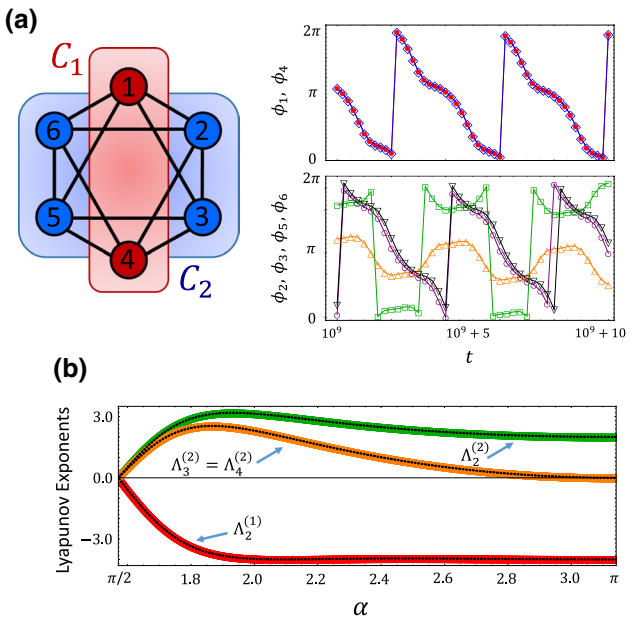

Fig. 1 **a** Left: schematic diagram of the network used in this paper. Right: $\phi_1(\Diamond)$, ϕ_4 (filled circle), ϕ_2 (unfilled circle), ϕ_3 ($\square$), $\phi_5(\nabla)$, and $\phi_6(\triangle)$ of the chimera state observed in the network. To observe this state, we integrate Eq. (2) with $\alpha = 1.58$ for a random initial condition $(\phi_1, \ldots, \phi_6) \in [0, 2\pi)^6$ at $t = -10^3$ to set t to zero after an initial transient. (Note that the chimera state is observed for $t \geq 0$ in Fig. 2.) **b** Thick lines indicate numerically estimated transverse Lyapunov exponents $\Lambda_\kappa^{(m)}$ for each cluster C_m. To obtain these lines, we integrate Eq. (6) with Eq. (4) up to $t = 10^5$ for each α. To discard the initial transient, we numerically integrate Eq. (4) over $-10^5 \leq t \leq 0$ for randomly taken $s_m(-10^5) \in [0, 2\pi)$ $(m = 1, 2)$ to obtain $s_1(0)$ and $s_2(0)$ for each α. Dotted lines indicate the functional form of $\Lambda_\kappa^{(m)}(\alpha)$ discussed in the main text

phase of the first cluster by s_1 and that of the second cluster by s_2. Then, the time derivatives of s_1 and s_2 are, respectively, given by

$$\begin{aligned} \dot{s}_1(t) =& \sin(\phi_2(t) - s_1(t) + \alpha) + \sin(\phi_3(t) - s_1(t) + \alpha) \\ &+ \sin(\phi_5(t) - s_1(t) + \alpha) + \sin(\phi_6(t) - s_1(t) + \alpha), \\ \dot{s}_2(t) =& 2\sin(\alpha) + \sin(\phi_1(t) - s_2(t) + \alpha) \\ &+ \sin(\phi_4(t) - s_2(t) + \alpha). \end{aligned} \tag{3}$$

Therefore, the synchronous phase of each cluster evolves following Eq. (3), meaning that each cluster can be synchronous irrespective of the oscillator phases of the other cluster.

2.3 Observation of a chimera state where only one cluster is synchronized

A chimera state of synchronized C_1 and desynchronized C_2 is discovered using the following procedure. (i) We avoid the complete phase synchronization of all six oscillators by using $\alpha \in (\pi/2, \pi)$ in which complete phase synchronization is unstable. (ii) In this range of α, we integrate

the quotient network dynamics of Eq. (2) for the two synchronous clusters C_1 and C_2 and show that the synchronous state of C_1 is stable, whereas that of C_2 is unstable along the trajectory of the two synchronous clusters. (iii) Finally, we observe the chimera state in the range of α by integrating the governing equation (Eq. (2)) for random initial phases.

We consider the quotient network dynamics of Eq. (2) for the two synchronous clusters C_1 and C_2 given by

$$\begin{aligned}\dot{s}_1(t) =& 4\sin(s_2(t) - s_1(t) + \alpha)\\ \dot{s}_2(t) =& 2\sin(s_1(t) - s_2(t) + \alpha) + 2\sin(\alpha),\end{aligned} \tag{4}$$

where s_1 and s_2 are the phases of the synchronous clusters C_1 and C_2, respectively (i.e. $s_1 = \phi_1 = \phi_4$ and $s_2 = \phi_2 = \phi_3 = \phi_5 = \phi_6$). A variational equation of Eq. (4) along the trajectory of complete phase synchronization $s(t) = s_1(t) = s_2(t)$ is given by

$$\dot{\eta}(t) = -6\cos(\alpha)\eta(t) \tag{5}$$

for $s_1(t) = s(t) - 2\eta(t)$ and $s_2(t) = s(t) + \eta(t)$. We find that $\eta(t)$ diverges for $\pi/2 < \alpha < \pi$ such that complete phase synchronization is unstable and therefore avoided. Accordingly, the phases of the two synchronous clusters remain distinct ($s_1(t) \neq s_2(t)$) in the range $\pi/2 < \alpha < \pi$.

Along the trajectory $(s_1(t), s_2(t))$ of Eq. (4) for $\pi/2 < \alpha < \pi$, we show that the synchronous state of C_1 is stable whereas that of C_2 is unstable. For the deviation of each phase $\delta\phi_i = \phi_i - s_m$ for $i \in C_m$ ($m = 1, 2$), we consider perturbation transverse to the synchronization manifold of each cluster. Specifically, we consider perturbations $\eta_\kappa^{(1)}$ ($\kappa = 2$) for C_1 and $\eta_\kappa^{(2)}(\kappa = 2, 3, 4)$ for C_2, where $\eta_2^{(1)} = (\delta\phi_1 - \delta\phi_4)/\sqrt{2}$, $\eta_2^{(2)} = (-\delta\phi_2 + \delta\phi_3 - \delta\phi_5 + \delta\phi_6)/2$, $\eta_3^{(2)} = (\delta\phi_2 - \delta\phi_5)/\sqrt{2}$ and $\eta_4^{(2)} = (\delta\phi_3 - \delta\phi_6)/\sqrt{2}$. Then, variational equations of Eq. (2) along $\phi_i = s_m$ for $i \in C_m$ ($m = 1, 2$) are given by

$$\begin{aligned}\dot{\eta}_2^{(1)}(t) =& -4\cos(s_2(t) - s_1(t) + \alpha)\eta_2^{(1)}(t),\\ \dot{\eta}_2^{(2)}(t) =& -2\big[\cos(s_1(t) - s_2(t) + \alpha) + 2\cos(\alpha)\big]\eta_2^{(2)}(t),\\ \dot{\eta}_3^{(2)}(t) =& -2\big[\cos(s_1(t) - s_2(t) + \alpha) + \cos(\alpha)\big]\eta_3^{(2)}(t),\\ \dot{\eta}_4^{(2)}(t) =& -2\big[\cos(s_1(t) - s_2(t) + \alpha) + \cos(\alpha)\big]\eta_4^{(2)}(t).\end{aligned} \tag{6}$$

We numerically obtain transverse Lyapunov exponents $\Lambda_\kappa^{(m)} = (1/t)\ln(||\eta_\kappa^{(m)}(t)||/||\eta_\kappa^{(m)}(0)||)$ for $t \gg 1$, as shown in Fig. 1b. We note that $\Lambda_3^{(2)} = \Lambda_4^{(2)}$ from Eq. (6).

We can obtain a functional form of $\Lambda_\kappa^{(m)}$ depending on α by using the evolving $s_1(t)$ and $s_2(t)$ of Eq. (4) with a time-independent phase difference $Y = s_1(t) - s_2(t)$. If we insert $Y = s_1(t) - s_2(t)$ into Eq. (4) with $\dot{s}_1 = \dot{s}_2$, we can derive Y as a function of α such that $Y(\alpha) = \cos^{-1}\big[(-4 - 5\cos(2\alpha))/(5 + 4\cos(2\alpha))\big]$. Then, we obtain a functional form of $\Lambda_\kappa^{(m)}(\alpha)$ from Eq. (6) by using the relation $\dot{\eta}_\kappa^{(m)}(t) = \Lambda_\kappa^{(m)}(\alpha)\eta_\kappa^{(m)}(t)$. We check that this analytic form of $\Lambda_\kappa^{(m)}(\alpha)$ agrees well with the numerical result, as shown in Fig. 1b.

For $\pi/2 < \alpha < \pi$ where complete phase synchronization (i.e. $\phi_i(t) = s(t)$ for $\forall i$) is avoided, we find that $\Lambda_2^{(1)} < 0$, $\Lambda_2^{(2)} > 0$ and $\Lambda_3^{(2)} = \Lambda_4^{(2)} > 0$ as in Fig. 1b such that the synchronous state of C_1 is stable while that of C_2 is unstable along the trajectory $s_1(t) \neq s_2(t)$ of Eq. (4). Therefore, we expect the chimera state to be observed in the range $\pi/2 < \alpha < \pi$ using random initial conditions of ϕ_i for which only the oscillators in C_1 will synchronize spontaneously. Via numerical integration of Eq. (2), we indeed observe that the chimera state persists even after $t = 10^9$ for a random initial condition with $\alpha \in (\pi/2, \pi)$, as shown in the right panel of Fig. 1a.

We remark that the chimera state is found with finite probability for random initial conditions and that other states can also be observed depending on the initial conditions (Sect. 3).

2.4 The trajectory of the phase differences of the desynchronized oscillators relative to the synchronous cluster is a stable periodic orbit

To show that the chimera state in the right panel of Fig. 1a is persistent, we demonstrate the periodic behavior of the state. At first, we obtain numerically that $\dot{\phi}_i(t + T) = \dot{\phi}_i(t)$ ($i = 1, 2, 4, 5$) and $\dot{\phi}_i(t + 2T) = \dot{\phi}_i(t)$ ($i = 3, 6$) for $t \geq 0$ with constant $T \approx 2.02$, as shown in Fig. 2. We note that the least common multiple of the periods of all $\dot{\phi}_i$ is $2T$. This periodic behavior might be understood analytically by finding the integral of the motion for this state [10].

As previously mentioned, in the chimera state, two oscillators $C_1 = \{1, 4\}$ are phase synchronized, while the other four oscillators $C_2 = \{2, 3, 5, 6\}$ are desynchronized. A necessary condition for phase synchronization of the two oscillators $\{i, j\}$ over a (finite) interval of t is $\dot{\phi}_i(t) = \dot{\phi}_j(t)$ over the interval of t. Based on the numerical results in Fig. 2, no pair of oscillators $\{i, j\}$ for $1 \leq i \neq j \leq 6$ satisfies $\dot{\phi}_i(t) = \dot{\phi}_j(t)$ over the common period $2T$ except the pair $C_1 = \{1, 4\}$, which repeats every $2T$. Therefore, the chimera state where only the pair $C_1 = \{1, 4\}$ is phase synchronized will persist permanently.

Based on the numerical results, $\phi_i(t)$ are quasiperiodic functions obeying $\phi_i(t + 2T) = \phi_i(t) + k_i$ for some constants k_i. If we conjecture that $k_i = k$ for $\forall i$ (i.e., $\phi_i(t + T) = \phi_i(t) + k/2$ $(i = 1, 2, 4, 5)$) with $\phi_3(t + T) = \phi_6(t) + k/2$, the periodic behavior of $\dot{\phi}_i(t)$ can be derived using Eq. (2) consistently. In this condition, the trajectory of the phase differences of the four desynchronized oscillators relative to the synchronous cluster given

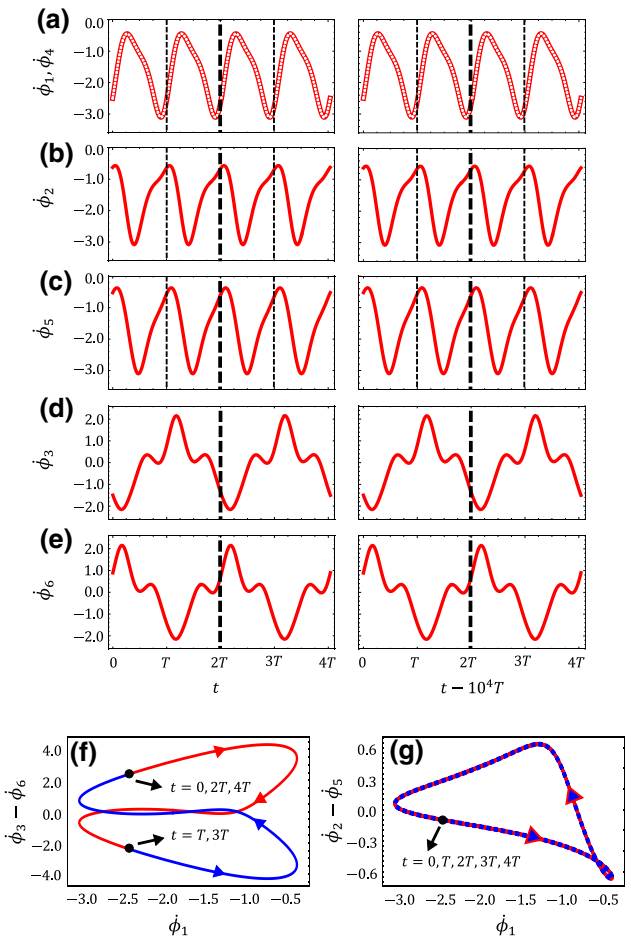

Fig. 2 Periodicity in the time series of $\dot{\phi}_i(t)$ of the chimera state in Fig. 1a. Numerical data to support that **a** $\dot{\phi}_1$ (solid line) and $\dot{\phi}_4$ (dotted line), **b** $\dot{\phi}_2$, and **c** $\dot{\phi}_5$ are periodic functions with period T. Comparison between the left and right panels in each row shows that the same pattern of $\dot{\phi}_i(t)$ $(i = 1, 2, 4, 5)$ during period T appears after 10^4 cycles. Numerical data to support that **d** $\dot{\phi}_3$ and **e** $\dot{\phi}_6$ are periodic functions with period $2T$. Comparison between the left and right panels in each row shows that the same pattern of $\dot{\phi}_i(t)$ $(i = 3, 6)$ during period $2T$ appears after 5×10^3 cycles. **f** $(\dot{\phi}_1, \dot{\phi}_3 - \dot{\phi}_6)$ and **g** $(\dot{\phi}_1, \dot{\phi}_2 - \dot{\phi}_5)$ for $\dot{\phi}_i$ in the left panels of (**a**–**e**). $(\dot{\phi}_1, \dot{\phi}_3 - \dot{\phi}_6)$ moves around a fixed path two times with period $2T$, whereas $(\dot{\phi}_1, \dot{\phi}_2 - \dot{\phi}_5)$ moves around a fixed path four times with period T. Arrows indicate the direction of motion. These results support that the least common multiple of the periods of all $\dot{\phi}_i$ is indeed $2T$

by $\boldsymbol{\gamma}(t) = (\phi_2 - s_1, \phi_3 - s_1, \phi_5 - s_1, \phi_6 - s_1) \in [0, 2\pi)^4$ for $s_1 = \phi_1 = \phi_4$ is a periodic orbit of period $2T$. We check that the trajectory is indeed a periodic orbit of period $2T$ in Fig. 3.

We use Floquet theory for the stability of periodic orbits [42] to analyze the stability of the chimera state. To do so, we obtain the Lyapunov exponents (real parts of the characteristic exponents) of the periodic orbit $\boldsymbol{\gamma}(t)$ numerically. To be specific, we consider a 4×4 fundamental matrix $\boldsymbol{\Phi}(t)$ satisfying $\dot{\boldsymbol{\Phi}}(t) = D\mathbf{f}(\boldsymbol{\gamma}(t))\boldsymbol{\Phi}(t)$ with $\boldsymbol{\Phi}(0) = \mathbf{I}_4$, where $\mathbf{f}$ is a function such that $\dot{\boldsymbol{\gamma}}(t) = \mathbf{f}(\boldsymbol{\gamma}(t))$.

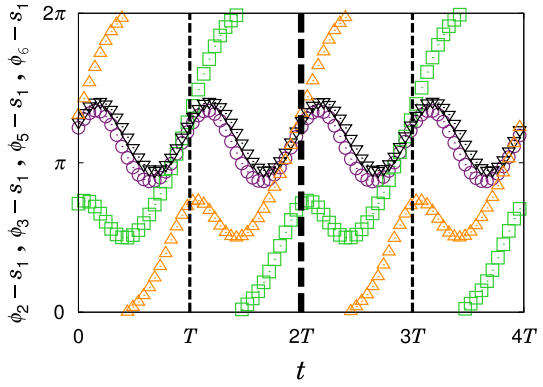

Fig. 3 $\phi_2 - s_1$ (unfilled circle), $\phi_3 - s_1$ (□), $\phi_5 - s_1$(▽), and $\phi_6 - s_1$(△) for $s_1 = \phi_1 = \phi_4$ of the chimera state in Fig. 1a

Then, we can obtain characteristic exponents λ_j by using the relation $e^{\lambda_j 2T} = \Lambda_j$, where Λ_j is the j-th eigenvalue of $\boldsymbol{\Phi}(2T)$. We note that $2T$ is the period of the orbit $\boldsymbol{\gamma}(t)$. A periodic orbit is known to have one zero Lyapunov exponent and to be stable if all the other Lyapunov exponents are negative. Here, as the numerically measured value of the second largest Lyapunov exponent of $\boldsymbol{\gamma}(t)$ is approximately -0.0028, the chimera state is stable.

Because of its periodic behavior, the chimera state that we observe is not chaotic [43], in contrast to the finite chimera state with $\alpha \in (0, \pi/2)$, which is chaotic before collapse to complete phase synchronization [7, 8, 18, 30]. Recently, several stable chaotic chimera states of finite size have been suggested using different types of oscillators [11, 13, 17].

3 Basin stability of the chimera state

For $\alpha \in (\pi/2, \pi)$, we measure the fraction of random initial conditions $(\phi_1(0), \ldots, \phi_6(0)) \in [0, 2\pi)^6$ that arrives at the chimera state following Eq. (2) (referred to as the basin stability of the chimera state). To be specific, we integrate Eq. (2) up to $t = 10^4$ for each initial condition and regard the final state as the chimera state if it satisfies the following two conditions: $\phi_1 = \phi_4$ and $\phi_i \neq \phi_j$ for any pairs $\{i, j\} \in \{1, 2, 3, 5, 6\}$ (as well as two other equivalent conditions given by the rotational symmetry of the network), and all $\dot{\phi}_i$ are periodic functions of t. For the latter, we regard each $\dot{\phi}_i$ as a periodic function if the standard deviation of the distances between two consecutive peak points of the function during $9 \times 10^3 \leq t \leq 10^4$ is less than the step-size of t used to integrate Eq. (2) numerically. Here, we take $t = 10^4$ for the upper limit of integration to measure basin stability after discarding the initial transients, because the chimera state in Fig. 1a appeared for a time interval of integration shorter than 10^3 beginning with a random condition.

We observe the chimera state with a finite probability for $\alpha < 1.633$, whereas no chimera state can be observed outside this range as shown in Fig. 4a–c. To understand the non-observance of the chimera state for $\alpha > 1.633$, we measure the second largest Lyapunov exponent of the chimera state (see Sect. 2.4) for $\alpha \in (\pi/2, 1.633)$, as shown in Fig. 4d. As previously mentioned, we find that the measured value is negative, such that the chimera state is stable. However, it drastically increases to zero as α approaches 1.633 from below, which supports the chimera state becoming unstable and thus non-observable as α exceeds 1.633.

In the entire range of $\pi/2 < \alpha < \pi$, we observe two other states as plotted in Fig. 4a, b. The trajectory of the state in Fig. 4a is $(\phi_1 = \phi_4 = \omega t + k_1,\ \phi_2 = \phi_5 = \omega t + k_1 + \pi,\ \phi_3 = k_2,\ \phi_6 = k_2 + \pi)$, and that of the state in Fig. 4b is given by $(\phi_1 = \phi_4 = \omega t + k_3,\ \phi_2 = \phi_5 = \omega t + 2\pi/3 + k_3,\ \phi_3 = \phi_6 = \omega t + 4\pi/3 + k_3)$ for arbitrary constants k_1, k_2, and k_3. Here, $\omega = -2\sin(\alpha)$ is derived for both states. We obtain the basin stability for these two states (considering other sets of trajectories given by the rotational and the reflectional symmetries of the network) as shown in Fig. 4c using the same upper limit of integration $t = 10^4$. We note that these two states are distinct from the chimera state in the sense that they, respectively, include two and three synchronous clusters, in contrast to the chimera state having only one synchronous cluster.

We understand roughly why the chimera state does not exist for $\alpha > 1.633$. We can show that the transverse Lyapunov exponent of both states in Fig. 4a, b is $2\cos(\alpha)$. This means that both states become more stable as α increases beyond the marginal value $\alpha = \pi/2$, where $2\cos(\alpha)$ for $\alpha > 1.633$ is much smaller than the measured Lyapunov exponents of the chimera state in Fig. 4d. Therefore, we expect the basin stability of the chimera state to shrink to zero for $\alpha > 1.633$.

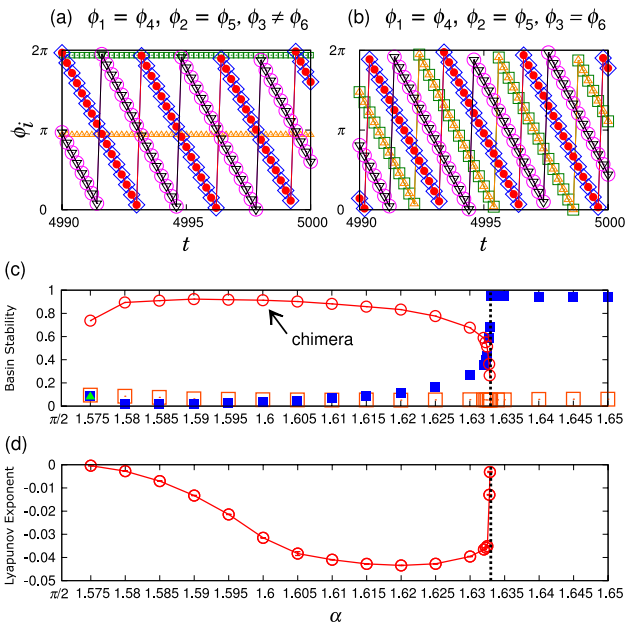

Fig. 4 Basin stability of the chimera state and other states. ϕ_1(◇), ϕ_2 (unfilled circle), ϕ_3 (□), ϕ_4 (filled circle), ϕ_5(▽), and ϕ_6(△) of **a** a state composed of two synchronous clusters ($\{1,4\}$, $\{2,5\}$) and an asynchronous cluster ($\{3,6\}$), and (b) a state composed of three synchronous clusters ($\{1,4\}$, $\{2,5\}$, $\{3,6\}$). We use $\alpha = 1.58$ to obtain these two states. **c** Basin stability of the chimera state (unfilled circle) and the two states in **a** (■) and **b** (□) versus α. For each value of α, we use 10^4 random initial conditions. The vertical dotted line at 1.633 indicates where the chimera state is no longer observed in the range of α to the right of the line. For each value of α, only the symbols of the states with nonzero basin stability are marked. For $\alpha = 1.575$, we observe states other than the chimera state and the two states in **a** and **b** (▲). **d** The average of the second largest Lyapunov exponents of the chimera states observed in (c) for each value of α. Error bars (standard deviations) are within the symbol size. The second largest Lyapunov exponent is approximately −0.0004 for $\alpha = 1.575$

4 Discussion

In this paper, we have discussed phase synchronization $\phi_i = \phi_j$ of oscillators $i \neq j$. From the perspective of phase synchronization, we observed a chimera state in the network depicted in Fig. 1a, where six oscillators are partitioned into a synchronous cluster $C_1 = \{1,4\}$ and an asynchronous cluster $C_2 = \{2,3,5,6\}$. Previously, a study [9] considered frequency synchronization $\Omega_i = \Omega_j$ of oscillators $i \neq j$, where the frequency of each oscillator i is given by $\Omega_i = \lim_{t\to\infty} \frac{1}{t}\int_0^t \dot{\phi}_i(t')\mathrm{d}t'$. From the perspective of frequency synchronization, the authors introduced the so-called weak chimera state for oscillators i, j, k in which $\Omega_i \neq \Omega_j$ and $\Omega_i = \Omega_k$. In the invariant subspace of the three-oscillator quotient system ($\phi_1 = \phi_4, \phi_2 = \phi_6, \phi_3 = \phi_5$) of Eq. (2) with the same network, they reported a weak chimera state where $\Omega_2 \neq \Omega_1$ and $\Omega_2 = \Omega_3$. Such existence of weak chimera states in three-oscillator quotient systems has recently been understood analytically [10].

In the present work, we numerically measure $\Omega_i = \frac{1}{t}\int_0^t \dot{\phi}_i(t')\mathrm{d}t'$ of the chimera state in Fig. 1a as $\Omega_i = -1.61081 \pm 0.00001$ $(i = 1,2,4,5)$ and $\Omega_i = -0.05504 \pm 0.00002$ $(i = 3,6)$ by integrating $\dot{\phi}_i$ up to $t = 10^5$. Based on the obtained values of Ω_i, we assume that the oscillators in the chimera state might be partitioned into the two clusters $\{1,2,4,5\}$ and $\{3,6\}$, where the oscillators in each cluster have the same value of Ω_i. Consequently, the chimera state will be a weak chimera state satisfying $\Omega_1 \neq \Omega_3$ and $\Omega_1 = \Omega_2$ in the invariant subspace of this five-oscillator quotient system ($\phi_1 = \phi_4, \phi_2, \phi_3, \phi_5, \phi_6$). We may understand the existence of the chimera state analytically by extending the analysis in previous works [9, 10] to the invariant subspace of this five-oscillator quotient system.

Finally, we note that the persistence of the synchronous state of the one subset irrespective of the asynchronous

phases of the other subset in the chimera state is related to the invariance of the adjacency matrix (symmetry) under permutations within the synchronous subset [17, 38–40]. The number of permutations conserving an adjacency matrix usually increases drastically with increasing network size [44]; therefore, we expect that the formation of synchronous subsets in diverse chimera states in large networks can be understood from the perspective of symmetry under permutations within each subset.

Acknowledgements This work was supported by National Research Foundation of Korea (NRF) Grant (No. 2017R1C1B1004292 and No. 2020R1F1A1061326).

References

1. M.J. Panaggio, D.M. Abrams, Nonlinearity **28**, R67 (2015)
2. O.E. Omel'chenko, Nonlinearity **31**, R121 (2018)
3. Y. Kuramoto, D. Battogtokh, Nonlinear Phenom. Complex Syst. **5**, 380 (2002)
4. D.M. Abrams, S.H. Strogatz, Phys. Rev. Lett. **93**, 174102 (2004)
5. D.M. Abrams, S.H. Strogatz, Int. J. Bifurcation Chaos Appl. Sci. Eng. **16**(1), 21 (2006)
6. D.M. Abrams, R. Mirollo, S.H. Strogatz, D.A. Wiley, Phys. Rev. Lett. **101**, 084103 (2008)
7. O.E. Omel'chenko, M. Wolfrum, Y.L. Maistrenko, Phys. Rev. E **81**, 065201(R) (2010)
8. M. Wolfrum, O.E. Omel'chenko, Phys. Rev. E **84**, 015201(R) (2011)
9. P. Ashwin, O. Burylko, Chaos **25**, 013106 (2015)
10. M. Thoubaan, P. Ashwin, Chaos **28**, 103121 (2018)
11. C. Bick, P. Ashwin, Nonlinearity **29**, 1468 (2016)
12. Y. Maistrenko et al., Phys. Rev. E **95**, 010203(R) (2017)
13. Y. Suda, K. Okuda, Phys. Rev. E **92**, 060901(R) (2015)
14. M.J. Panaggio, D.M. Abrams, P. Ashwin, C.R. Laing, Phys. Rev. E **93**, 012218 (2016)
15. N.I. Semenova, G.I. Strelkova, V.S. Anishchenko, A. Zakharova, Chaos **27**, 061102 (2017)
16. A.E. Botha, Sci. Rep. **6**, 29213 (2016)
17. Y.S. Cho, T. Nishikawa, A.E. Motter, Phys. Rev. Lett. **119**, 084101 (2017)
18. M. Wolfrum, O.E. Omel'chenko, S. Yanchuk, Y.L. Maistrenko, Chaos **21**, 013112 (2011)
19. G. Bordyugov, A. Pikovsky, M. Rosenblum, Phys. Rev. E **82**, 035205(R) (2010)
20. O.E. Omel'chenko, Nonlinearity **26**, 2469 (2013)
21. A. Mihara, R.O. Medrano-T, Nonlinear Dyn. **98**, 539 (2019)
22. I. Omelchenko, Y. Maistrenko, P. Hövel, E. Schöll, Phys. Rev. Lett. **106**, 234102 (2011)
23. K. Höhlein, F.P. Kemeth, K. Krischer, Phys. Rev. E **100**, 022217 (2019)
24. A.M. Hagerstrom et al., Nat. Phys. **8**, 658 (2012)
25. M.R. Tinsley, S. Nkomo, K. Showalter, Nat. Phys. **8**, 662 (2012)
26. E.A. Martens, S. Thutupalli, A. Fourrière, O. Hallatschek, Proc. Natl. Acad. Sci. USA **110**, 10563 (2013)
27. C. Meena, K. Murali, S. Sinha, Int. J. Bifurcation Chaos **26**, 1630023 (2016)
28. J.D. Hart, K. Bansal, T.E. Murphy, R. Roy, Chaos **26**, 094801 (2016)
29. D.P. Rosin et al., Phys. Rev. E **90**, 030902(R) (2014)
30. A. Banerjee, D. Sikder, Phys. Rev. E **98**, 032220 (2018)
31. F. Böhm, A. Zakharova, E. Schöll, K. Lüdge, Phys. Rev. E **91**, 040901(R) (2015)
32. A. Röhm, F. Böhm, K. Lüdge, Phys. Rev. E **94**, 042204 (2016)
33. L. Larger, B. Penkovsky, Y. Maistrenko, Nat. Commun. **6**, 7752 (2015)
34. J. Wojewoda, K. Czolczynski, Y. Maistrenko, T. Kapitaniak, Sci. Rep. **6**, 34329 (2016)
35. M.H. Matheny et al., Science **363**, eaav7932 (2019)
36. F.P. Kemeth et al., Chaos **26**, 094815 (2016)
37. H. Sakaguchi, Y. Kuramoto, Prog. Theor. Phys. **76**, 576 (1986)
38. V. Nicosia et al., Phys. Rev. Lett. **110**, 174102 (2013)
39. L.M. Pecora et al., Nat. Commun. **5**, 4079 (2014)
40. F. Sorrentino et al., Sci. Adv. **2**, e1501737 (2016)
41. P.J. Menck, J. Heitzig, N. Marwan, J. Kurths, Nat. Phys. **9**, 89 (2013)
42. L. Perko, *Differential Equations and Dynamical Systems*, 2nd edn. (Springer, Berlin, 1996)
43. C. Bick et al., Phys. Rev. Lett. **107**, 244101 (2011)
44. B.D. MacArthur, R.J. Sánchez-García, J.W. Anderson, Discrete Appl. Math. **156**, 3525 (2008)